Available online at www.sciencedirect.com

SciVerse ScienceDirect

Ceramics International 39 (2013) 7545–7549

CERAMICS INTERNATIONAL

www.elsevier.com/locate/ceramint

A novel synthesis route to $Sn_{1-x}RE_xO_{2-x/2}$ nanorods via microwave-induced salt-assisted solution combustion process

Weifan Chen[a,*], Ming Liu[a], Yucui Lin[a], Yue Liu[a], Lixing Yu[a], Ting Li[a], Jianming Hong[b,**]

[a]School of Materials Science and Engineering, Nanchang University, Nanchang 330031, PR China
[b]Center of Materials Analysis, Nanjing University, Nanjing 210093, PR China

Received 1 November 2012; received in revised form 5 February 2013; accepted 5 March 2013
Available online 14 March 2013

Abstract

$Sn_{1-x}RE_xO_{2-x/2}$ (RE=Y, La, Gd and Nd) nanorods have been prepared by annealing the as-obtained products from microwave-induced KCl-assisted solution combustion reaction. The phase evolution in the synthesis process was investigated by an X-ray diffractometer. Accordingly, the possible growth mechanism of $Sn_{1-x}RE_xO_{2-x/2}$ nanorods was discussed based on oriented attachment by polar forces. The results showed that the $Sn_{0.8}Y_{0.2}O_{1.9}$ nanorods were rutile-structured single crystals with 8–12 nm diameter and 100–200 nm length. Proper addition of KCl into the redox mixture solution is critical to the formation of $Sn_{1-x}RE_xO_{2-x/2}$ nanorods. The approach is convenient, inexpensive and efficient for the high yield preparation of $Sn_{1-x}RE_xO_{2-x/2}$ nanorods.

Keywords: A. Powders: Chemical preparation; B. Microstructure—final; D. Tin-based oxide nanorods

1. Introduction

As an n-type semiconductor with a wide tunable band gap, SnO_2 and SnO_2-based 1-D nanomaterials show great promise for their wide applications in gas sensors [1], transparent conducting electrodes [2], transistors [3], solar cells [4], Li ion batteries [5] and catalysts [6]. Many attempts have been devoted to fabricate SnO_2-based 1-D nanostructures via a variety of synthesis approaches, such as thermal decomposition/evaporation [7,8], hydro/solvothermal methods [9,10], template-based methods [11], and salt-assisted methods [12–16].

Although the salt-assisted routes for fabrication of SnO_2-based nanorods have been investigated, much improvement should still be made in fabricating SnO_2 nanorods in the rapid, high-yield, low-cost and environmentally-friendly ways. To the best of our knowledge, currently, some complicated synthesis procedures have been used for the fabrication, in which formation of the micro-emulsion or gel precursors [12,13], expensive surfactants [13,16] or complex [14], fine raw materials prepared ahead [14,15], higher temperature annealing with larger amounts of salt [13–16], and tedious grinding [15,16] may be required. Solution combustion synthesis has been regarded as a promising method for the preparation of nanomaterials [17]. To inhibit crystallite agglomeration and control the microstructures of the combustion-derived products, we developed an alternative strategy named as salt-assisted solution combustion synthesis, by which many novel nanostructured oxides have been easily fabricated [18,19]. In this paper, we thus report a simple and easy synthesis route for $Sn_{1-x}RE_xO_{2-x/2}$ nanorods via microwave-induced salt-assisted solution combustion combined with subsequent annealing, and discuss the possible growth mechanism. The method greatly reduces annealing temperature and salt amount. In addition, neither high pressure and grinding nor formation of the micro-emulsion or gel in the presence of expensive surfactants is necessary.

*Corresponding author. Tel.: +86 0791 83969553; fax: +86 0791 83969329.
**Corresponding author. Tel.: +86 025 86205529; fax: +86 025 83325180.
E-mail addresses: weifan-chen@163.com (W. Chen), jianming_hong@163.com (J. Hong).

0272-8842/$ - see front matter © 2013 Elsevier Ltd and Techna Group S.r.l. All rights reserved.
http://dx.doi.org/10.1016/j.ceramint.2013.03.006

2. Experimental procedure

Initially, the required amounts of RE_2O_3 (RE=Y, La, Gd and Nd) were dissolved into nitric acid to obtain corresponding rare earth nitrate solution, into which the desired molar ratios of $SnCl_4{\cdot}5H_2O$, NH_4NO_3, KCl and ethylene glycol were dissolved and mixed by stirring and heating. Afterwards, the transparent solution was condensed and transferred into a microwave oven to induce self-propagating solution combustion. After the combustion-derived precursor was annealed in a muffle furnace at 400 °C for 4 h, the obtained powder was washed with hot deionized water and dried at 60 °C for 4 h to obtain $Sn_{1-x}RE_xO_{2-x/2}$ samples.

The phases evolution of the samples was characterized by a Bruker D8-advance X-ray diffractometer with Cu Kα radiation (λ=1.5418 Å). The structure and morphology of the samples were analyzed by a JEOL JEM-2010 transmission electron microscope operating under 200 kV and a FEI Quanta 200F field emission scanning electron microscope. The selected area electron diffraction (SAED) patterns of the samples were also taken with a JEOL JEM-2010 transmission electron microscope.

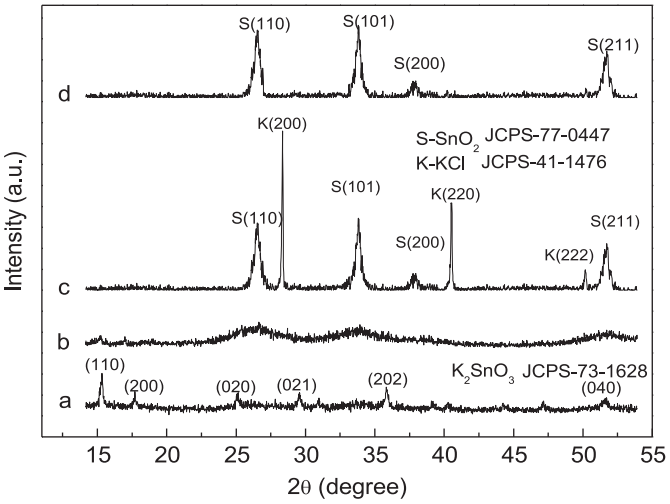

Fig. 1. X-ray diffraction patterns of the samples in the synthetic processes of $Sn_{0.8}Y_{0.2}O_{1.9}$ (α=1, β=0.5): (a) combustion-derived sample; (b) sample obtained after washing sample (a) and subsequent drying at 60 °C for 4 h; (c) sample obtained from annealing sample (a) at 400 °C for 4 h; and (d) sample obtained from washing sample (c) and subsequent drying at 60 °C for 4 h.

3. Results and discussion

According to the principle of propellant chemistry [20], the salt-assisted redox combustion reaction and subsequent annealing can be generally expressed as follows:

$$SnCl_4 + Y(NO_3)_3 + NH_4NO_3 + 17\alpha/10HOCH_2CH_2OH + 17(\alpha-1)/4O_2 + 5\beta KCl \rightarrow 5Sn_{0.8}Y_{0.2}O_{1.9} + 17\alpha/5CO_2 + 5/2N_2 + (2+51\alpha/10)H_2O + 16HCl + 5\beta KCl \quad (1)$$

In Eq. (1), α is termed as molar ratio of fuel-to-oxidants; α=1 means stoichiometric condition, whereas α>1 or <1 implies fuel rich or lean conditions, respectively. β represents the amount of KCl, which is expressed as the molar ratio of KCl to metal ions of $Sn_{1-x}RE_xO_{2-x/2}$. NH_4NO_3 was used as combustion-supporting agent.

As shown in Fig. 1(a), all diffraction peaks of sample (a) can be perfectly indexed to K_2SnO_3 structure (JCPDS-73-1628), indicating the presence of crystalline K_2SnO_3. We know that K_2SnO_3 is soluble in water; however, after aqueous washing of sample (a), there is still some residue dissoluble in water, which is referred to as sample (b). Fig. 1(b) presents very weak diffraction peaks corresponding to the characteristic diffraction peaks of SnO_2, indicating that sample (b) is amorphous $Sn_{0.8}Y_{0.2}O_{1.9}$. It is concluded that sample (a) consists of K_2SnO_3 nanocrystallites and amorphous $Sn_{0.8}Y_{0.2}O_{1.9}$ nanoparticles. Notably, no characteristic diffraction peaks of KCl in Fig. 1(a) can be observed, which may be due to the monolayer dispersion of KCl on the surface of the combustion-derived precursor nanoparticles [21]. However, after annealing of sample (a), the characteristic diffraction peaks corresponding to SnO_2 (JCPDS-77-0447) and KCl (JCPDS-41-1476) appear, as shown in Fig. 1(c). The appearance of characteristic diffraction peaks of KCl can be understood as follows: in the annealing process, $Sn_{0.8}Y_{0.2}O_{1.9}$ nanoparticles grow and their specific surface areas decrease; as a result, the amount of KCl is beyond the closed-pack monolayer dispersion capacity of KCl on the surface of the as-annealed particles [21]. Fig. 1(d) clearly indicates that sample (d) is only indexed to SnO_2 structure (JCPDS-77-0447) after aqueous washing of sample (c). No characteristic diffraction peaks of Y_2O_3 are observed in Fig. 1(d), revealing that Y^{3+} is uniformly doped into the SnO_2 matrix lattice.

Fig. 2(a) and (c) clearly shows that the products are entirely comprised of relatively uniform nanorods with 8–12 nm diameter and 150–200 nm length. The SAED pattern shown in the upper left inset of Fig. 2(a) indicates that the as-prepared $Sn_{0.8}Y_{0.2}O_{1.9}$ nanorods are single-crystals. The lattice fringes in Fig. 2(b) further confirm the single-crystalline structure of $Sn_{0.8}Y_{0.2}O_{1.9}$ nanorods and reveal that the preferential growth direction is [001]. The distance between adjacent lattice fringes corresponding to (110) interplanar spacing of rutile $Sn_{0.8}Y_{0.2}O_{1.9}$ is 0.342 nm, larger than rutile SnO_2 due to the doping of Y^{3+}. Fig. 2(d) presents TEM of the products derived from KCl-assisted solution combustion process prior to annealing. It reveals that the products are composed of well-dispersed nanoparticles, which are favorable for the formation of nanorods in the molten salt during annealing. The SAED pattern shown in the upper left inset of Fig. 2(d) indicates that the combustion -derived products are amorphous, which is in agreement with X-ray diffraction patterns. In a sharp contrast with the case in the presence of KCl, Fig. 2(e) shows that the annealed products in the absence of KCl are inseparable three-dimensional porous nanocrystallite aggregates. The ring-type SAED pattern in the upper left inset of Fig. 2(e) also confirms that the aggregates are polycrystalline. Therefore, the introduction of KCl in solution combustion synthesis has great influence on the sample morphology, thus resulting in the formation of nanorods.

In the process of microwave-induced KCl-assisted solution combustion, the self-propagating solution combustion reaction releases a large amount of heat in a very short time; except one

small part of KCl reacting with Sn^{4+}, the left part precipitates in situ instantly to form a thin film on the surface of the nanoparticles derived from combustion with diminishing free enthalpy. Under the proper conditions, the monolayer dispersion of KCl occurs on the surface of the nanoparticles, leading to disappearance of characteristic diffraction peaks of KCl, which is shown in Fig. 1(a). Hence, the combustion-derived products are composed of KCl-coated nanoparticles, which are ideal for post-heating. Because the melting point for a given nanostructure can be one-third of its bulk melting point, and the adopted 400 °C is higher than one-third of the melting point of bulk KCl (770 °C), a favorable flux environment for the growth of nanorods can be achieved when the KCl-coated nanoparticles are annealed at 400 °C.

The specific surface energies of crystalline SnO_2 have been calculated by different methods. The calculations show the same general sequence in the order of increasing energy, i.e., (110)< (100)<(101)<(001) [22], suggesting that the (110) and (001) surfaces have the lowest and the highest surface energies, respectively. Therefore, the [001] and [110] directions are the most favored and the least favored growth directions, respectively. As a consequence, SnO_2 crystallites tend to grow along the [001] direction, resulting in the formation of one-dimensional single-crystalline nanostructures, especially in the molten salt. Our experimental results are in good agreement with these calculations.

The growth mechanism of the nanorods can be also understood based on oriented attachment by polar forces [23]. That is, firstly, the microwave-induced solution combustion reaction occurs with huge release of heat and gases, resulting in a drastic temperature increase, and the salt precipitation in situ is completed in an instant to form a coat of salt on the surface of the newly-formed precursor nanoparticles; in the subsequent annealing process, the as-derived amorphous $Sn_{1-x}RE_xO_{2-x/2}$ and crystalline K_2SnO_3 nanoparticles transform into $Sn_{1-x}RE_xO_{2-x/2}$ nanocrystallites. In the presence of molten KCl, $Sn_{1-x}RE_xO_{2-x/2}$ nanocrystallites rotate, rearrange and aggregate to minimize the surface energy by oriented attachment; finally, due to the highest specific surface energy of (001) crystal plane, the nanocrystallite aggregation can be further

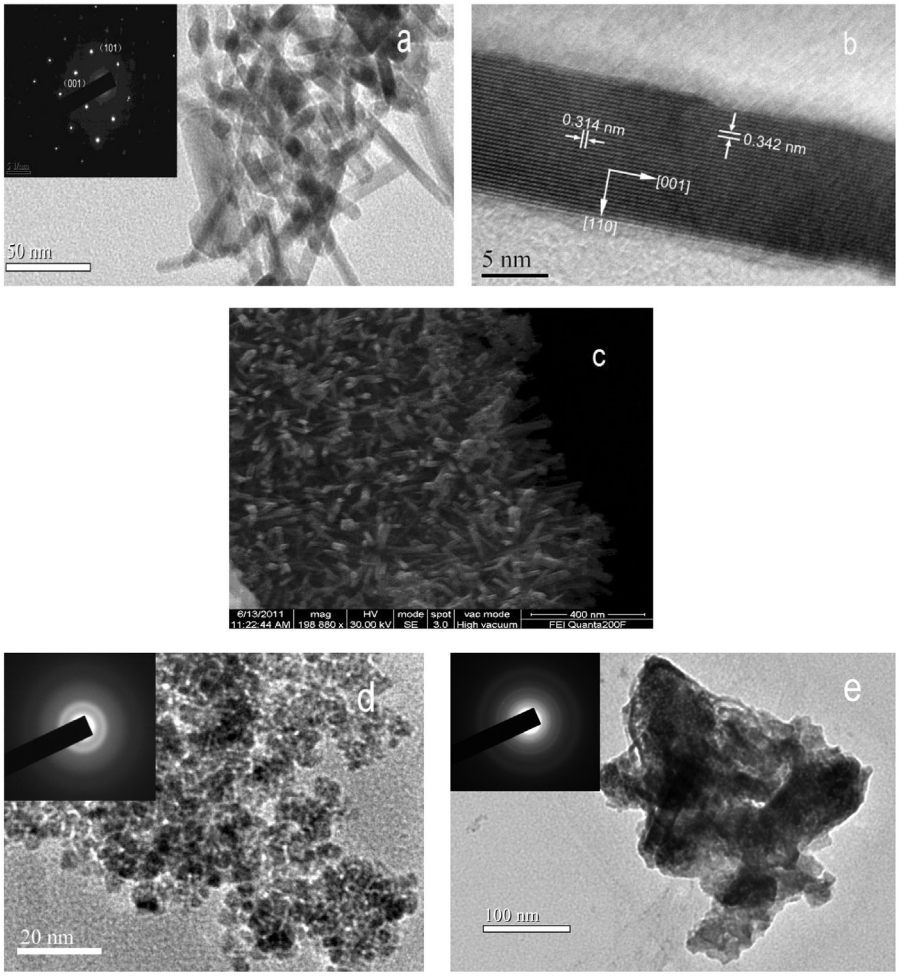

Fig. 2. (a) Transmission electron micrograph (TEM), (b) high-resolution TEM and (c) scanning electron micrograph (SEM) of $Sn_{0.8}Y_{0.2}O_{1.9}$ obtained from KCl-assisted solution combustion process ($\alpha=1$, $\beta=0.5$, 400 °C, 4 h); (d) TEM of the products derived from KCl-assisted solution combustion process prior to annealing ($\alpha=1$, $\beta=0.5$). (e) TEM of $Sn_{0.8}Y_{0.2}O_{1.9}$ obtained from salt-free solution combustion process ($\alpha=1$, $\beta=0$, 400 °C, 4 h). The upper left insets of Fig. 2 (a), (d) and (e) are the selected area electron diffraction patterns from an individual nanorod with a [1–10] zone axis, nanoparticles and nanocrystallite aggregates, respectively.

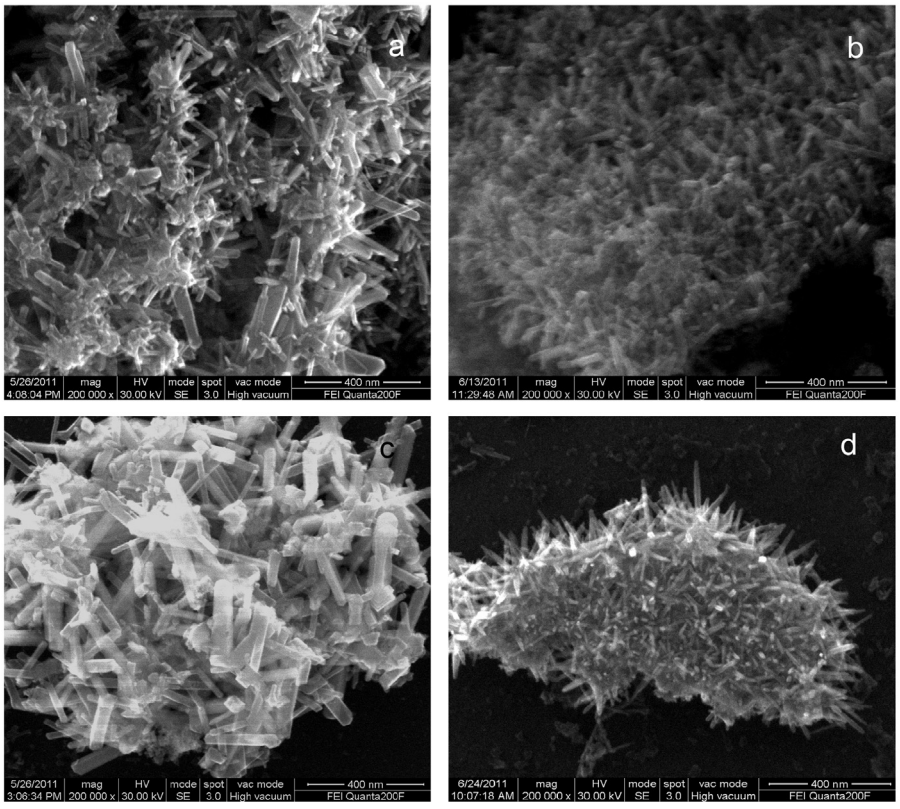

Fig. 3. Scanning electron micrographs of the obtained nanorods (α=1, β=0.5, 400 °C, 4 h): (a) SnO_2; (b) $Sn_{0.8}La_{0.2}O_{1.9}$; (c) $Sn_{0.8}Gd_{0.2}O_{1.9}$; and (d) $Sn_{0.8}Nd_{0.2}O_{1.9}$.

recrystallized and grows along the [001] direction to form nanorods with the assistance of molten KCl.

Moreover, the approach can be extended to the fabrication of SnO_2 and $Sn_{1-x}RE_xO_{2-x/2}$ nanorods by choosing proper salt and fuel, adjusting amount of salt and fuel, and tuning the duration and temperature of post-heating, as shown in Fig. 3(a–d).

4. Conclusions

We have developed a novel approach for the fabrication of $Sn_{1-x}RE_xO_{2-x/2}$ nanorods via microwave-induced KCl-assisted solution combustion and subsequent annealing. Each $Sn_{0.8}RE_{0.2}O_{1.9}$ nanorod is a single crystal with rutile structure and has a preferred [001] growth direction. The proper addition of KCl into the redox mixture solution is of critical importance for the preferred growth and formation of $Sn_{1-x}RE_xO_{2-x/2}$ nanorods, which is supposed to follow the oriented attachment mechanism by polar forces. The approach provides a convenient, inexpensive and efficient route for large-scale preparation of SnO_2-based nanorods.

Acknowledgments

This work was supported by the National Nature Science Foundation of China (No. 21061011) and the Scientific and Technological Research Project of Jiangxi Education Department (No. GJJ12034). The authors wish to thank Prof. Xiang Wang for his assistance in revising the English presentation of the manuscript.

References

[1] Q. Kuang, C.S. Lao, Z.L. Wang, Z.X. Xie, L.S. Zheng, High-sensitivity humidity sensor based on a single SnO_2 nannowire, Journal of the American Chemical Society 129 (2007) 6070–6071.
[2] Q. Wan, E.N. Dattoli, W. Lu, Transparent metallic Sb-doped SnO_2 nanowires, Applied Physics Letters 90 (2007) 222107–222110.
[3] J. Sun, H.X. Liu, J. Jiang, A.X. Lu, Q. Wan, Low-voltage transparent SnO_2 nanowire transistors gated by microporous SiO_2 solid-electrolyte with improved polarization response, Journal of Materials Chemistry C 20 (2010) 8010–8015.
[4] Q.F. Zhang, G.Z. Cao, Nanostructured photoelectrodes for dye-sensitized solar cells, Nano Today 6 (2011) 91–109.
[5] D.W. Kim, I.S. Hwang, S.J. Kwon, H.Y. Kang, K.S. Park, Y.J. Choi, K. J. Choi, J.G. Park, Highly conductive coaxial SnO_2–In_2O_3 heterostructured nanowires for Li ion battery electrodes, Nano Letters 7 (2007) 3041–3045.
[6] Y.T. Han, X. Wu, Y.L. Ma, L.H. Gong, F.Y. Qu, H.J. Fan, Porous SnO_2 nanowire bundles for photocatalyst and Li ion battery applications, Crystal Engineering Communications 13 (2011) 3506–3510.
[7] C. Xu, G. Xu, Y. Liu, X. Zhao, G. Wang, Preparation and characterization of SnO_2 nanorods by thermal decomposition of SnC_2O_4 precursor, Scripta Materialia 46 (2002) 789–794.
[8] H.W. Kim, S.H. Shim, Synthesis and characteristics of SnO_2 needle-shaped nanostructures, Journal of Alloys and Compounds 426 (2006) 286–289.
[9] B. Cheng, J.M. Russell, W.S. Shi, L. Zhang, E.T. Samulski, Large-scale, solution-phase growth of single-crystalline SnO_2 nanorods, Journal of the American Chemical Society 126 (2004) 5972–5973.

[10] X.F. Liu, J. Iqbal, Z.B. Wu, B. He, R.H. Yu, Structure and room-temperature ferromagnetism of Zn-doped SnO_2 nanorods prepared by solvothermal method, Journal of Physical Chemistry C 114 (2010) 4790–4796.
[11] L. Shi, Y.M. Xu, Q. Li, Controlled fabrication of SnO_2 arrays of well-aligned nanotubes and nanowires, Nanoscale 2 (2010) 2104–2108.
[12] D.W. Wang, X. Chu, M. Gong, Gas-sensing properties of sensors based on single-crystalline SnO_2 nanorods prepared by a simple molten-salt method, Sensors and Actuators B 117 (2006) 183–187.
[13] F. Gu, S.F. Wang, H.M. Cao, C.Z. Li, Synthesis and optical properties of SnO_2 nanorods, Nanotechnology 19 (2008) 095708–095712.
[14] Y. Wang, J.Y. Lee, T.C. Deivaraj, Controlled synthesis of V-shaped SnO_2 nanorods, Journal of Physical Chemistry B 108 (2004) 13589–13593.
[15] J.Q. Sun, J.S. Wang, X.C. Wu, G.S. Zhang, J.Y. Wei, S.Q. Zhang, H. Li, D.R. Novel, Method for high-yield synthesis of rutile SnO_2 nanorods by oriented aggregation, Crystal Growth and Design 6 (2006) 1585–1587.
[16] W.Z. Wang, C.K. Xu, X.S. Wang, Y.K. Liu, Y.J. Zhan, C.L. Zheng, F. Q. Song, G.H. Wang, Preparation of SnO_2 nanorods by annealing SnO_2 powder in NaCl flux, Journal of Materials Chemistry 12 (2002) 1922–1925.
[17] A.S. Mukasyan, Solution combustion as a promising method for the synthesis of nanomaterials, Advanced Sciences and Technologies 63 (2010) 187–196.
[18] W.F. Chen, F.S. Li, J.Y. Yu, L.L. Liu, H.L. Gao, Rapid synthesis of mesoporous ceria–zirconia solid solutions via a novel salt-assisted combustion process, Materials Research Bulletin 41 (2006) 2318–2324.
[19] W.F. Chen, J.M. Hong, Y.X. Li, Facile fabrication of perovskite single-crystalline $LaMnO_3$ nanocubes via a salt-assisted solution combustion process, Journal of Alloys and Compounds 484 (2009) 846–850.
[20] S.R. Jain, K.C. Adiga, V.R.P Vemeker, A new approach to thermo-chemical calculation of condensed fuel–oxidizer mixtures, Combustion and Flame 40 (1981) 71–76.
[21] Y.C. Xie, Y.Q. Tang, Spontaneous monolayer dispersion of oxides and salts onto surface of supports: applications to heterogeneous catalysis, Advances in Catalysis 37 (1990) l–47.
[22] J. Oviedo, M.J. Gillan, Energetics and structure of stoichiometric SnO_2 surfaces studied by first-principles calculations, Surface Science 463 (2000) 93–101.
[23] E.R. Leite, T.R. Giraldi, F.M. Pontes, E. Longo, A. Beltran, J. Andres, Crystal growth in colloidal tin oxide nanocrystals induced by coalescence at room temperature, Applied Physics Letters 83 (2003) 1566–1568.